



THE UNIVERSITY *of* EDINBURGH

Edinburgh Research Explorer

Validation of a blood plasma separation system by biomarker detection

Citation for published version:

Kersaudy-Kerhoas, M, Kavanagh, DM, Dhariwal, RS, Campbell, CJ & Desmulliez, MPY 2010, 'Validation of a blood plasma separation system by biomarker detection' Lab on a Chip, vol 10, no. 12, pp. 1587-1595., 10.1039/b926834k

Digital Object Identifier (DOI):

[10.1039/b926834k](https://doi.org/10.1039/b926834k)

Link:

[Link to publication record in Edinburgh Research Explorer](#)

Document Version:

Author final version (often known as postprint)

Published In:

Lab on a Chip

Publisher Rights Statement:

Copyright © 2010 by the Royal Society of Chemistry; all rights reserved.

General rights

Copyright for the publications made accessible via the Edinburgh Research Explorer is retained by the author(s) and / or other copyright owners and it is a condition of accessing these publications that users recognise and abide by the legal requirements associated with these rights.

Take down policy

The University of Edinburgh has made every reasonable effort to ensure that Edinburgh Research Explorer content complies with UK legislation. If you believe that the public display of this file breaches copyright please contact openaccess@ed.ac.uk providing details, and we will remove access to the work immediately and investigate your claim.



Post-print of peer-reviewed article published by the Royal Society of Chemistry.

Published article available at: <http://dx.doi.org/10.1039/B926834K>

Cite as:

Kersaudy-Kerhoas, M., Kavanagh, D. M., Dhariwal, R. S., Campbell, C. J., & Desmulliez, M. P. Y. (2010). Validation of a blood plasma separation system by biomarker detection. *Lab on a Chip*, 10(12), 1587-1595.

Manuscript received: 22/12/2009; Accepted: 03/03/2010; Article published: 31/03/2010

Validation of a blood plasma separation system by biomarker detection**

Maiwenn Kersaudy-Kerhoas,^{1,*} Deirdre M. Kavanagh,¹ Resham S. Dhariwal,¹ Colin J. Campbell^{2,3,*}
and Marc P. Y. Desmulliez¹

^[1]MicroSystems Engineering Centre (MISEC), School of Engineering & Physical Sciences, Heriot-Watt University, Earl Mountbatten Building, Edinburgh, U.K.

^[2]Division of Pathway Medicine, University of Edinburgh Medical School, Chancellor's Building, 49 Little France Crescent, Edinburgh, U.K.

^[3]EaStCHEM, School of Chemistry, Joseph Black Building, University of Edinburgh, West Mains Road, Edinburgh, EH9 3JJ, UK.

^[*]Corresponding authors; M.K.K. e-mail: mk87@hw.ac.uk; fax: +44 131 451 4155; tel: +44 131 451 4148; C.J.C. e-mail: colin.campbell@ed.ac.uk; fax: +44 131 650 6453; tel: +44 131 650 7546

^[**]The staff of the Division of Pathway Medicine, University of Edinburgh is thanked for their help in the preparation of the PCR reactions. We would like to thank Neil Johnston for access to the Centre for Cardiovascular Science, Queen's Medical Research Institute, Edinburgh, for cell counting. Shonna Johnston is thanked to allow access to the Flow Laboratory, Queen's Medical Research Institute, Edinburgh and for the provision of antibodies. Thank you to Tiina Kitari for providing flow check beads. Funding from the EPSRC 3DM-Integration Grand challenge project EP/C534212/1 is gratefully acknowledged. The manufacturing of the lab-on-a-chip was carried out by Epigem Ltd in the Fluence Microfluidics Application Centre supported by the Technology Strategy Board (TSB) and the ONE Regional Development Agency as part of the UK's MNT Network.

Keywords:

polymerase chain-reaction; whole human blood; free fetal dna; maternal plasma; cancer-patients; microfluidic device; circulating DNA; cross-flow; serum; cells

Abstract

A microfluidic system was developed for blood plasma separation at high flow rate. This system uses only hydrodynamic forces to separate red and white blood cells from whole blood. The microfluidic network features a series of constrictions and bifurcations to enhance the product yield and purity. A maximum purity efficiency of 100% is obtained on blood with entrance hematocrit level up to 30% with a flow rate of 2mL/hr. Flow cytometry was performed on the extracted plasma to evaluate the separation efficiency and to assess cell damage. A core target of this study was the detection of cell-free DNA from the on-chip extracted plasma. To this effect, PCR was successfully carried out off-chip on the cell-free DNA present in the plasma extracted on chip. The cell-free DNA was amplified without the need for purification after the separation, thereby showing the high quality of the plasma sample. The resulting data suggests that the system can be used as a preliminary module of a total analysis system for cell free DNA detection in human plasma.

Introduction

Blood Plasma separation on-chip

Optimum on-chip blood plasma separation techniques should have a high plasma yield, a large throughput and a high plasma purity, while keeping cellular damage to a minimum, such as not to contaminate the plasma with cellular DNA. On one hand, the miniaturization of centrifugation has been the topic of many research groups. Ducrée and Madou, for example, have utilised centrifugal forces developed through the rotation of their lab-on-CD devices to separate red blood cells from plasma^{1,2}. On the other hand, other researchers have focused on the development of a continuous separation method applicable to blood plasma separation. Jang et al developed a microfluidic network with a series of bifurcations ranging between 10 and 20µm in width. Faivre has used constrictions integrated before the bifurcation to increase the natural cell-free layer of blood flow at low Reynolds number³. Recently, Rodríguez-Villarreal et al. have demonstrated a high flow rate blood plasma separation device using one constriction and one bifurcation⁴. The biological validation of the resulting extracted plasma in terms of contamination was not however presented in this article.

In this paper we present a blood plasma extraction microsystem based on multiple constrictions in a microfluidic network together with the biological validation of this device through the detection of human cell free DNA (cfDNA) in the extracted plasma⁵. The chip overcomes certain limitations encountered in the literature as it runs at high-flow rate, high throughput, obtains a high level of plasma purity while causing very little cellular damage allowing thereby the extracted plasma to be

suitable for detection of cfDNA. In this regard, our microfluidic plasma separator can be regarded as a preliminary module to a low cost total analysis system for these types of applications⁶.

cfDNA

The existence of cell free DNA (cfDNA) in human plasma was first detected in cancer patients over 30 years ago⁷. However only in the last few years has its true diagnostic potential been realised resulting in an increasing interest in the detection and analysis of cfDNA^{8,9,10,11}. Potential applications of cfDNA detection include the diagnosis and prognosis of various malignancies^{8,9,11,12}, the monitoring of graft versus host disease after organ transplantation¹³ and non invasive prenatal diagnosis (NIPD)¹⁴. For the latter, cell free foetal DNA, cffDNA, is not only used today to diagnose gender-linked conditions¹⁵ or foetal rhesus D status^{16,17} but cffDNA is also employed as an indicator for pregnancy associated diseases such as pre-eclampsia and preterm labour¹⁸.

Analysis of cfDNA from plasma by PCR

Analysis of cfDNA first requires the separation of plasma or serum from whole blood. Purification is mostly required to remove the major inhibitors of the Polymerase Chain Reaction (PCR). These include natural components such as heme and immunoglobulin G and exogenous components such as anticoagulants²⁸. Furthermore, the plasma must be completely free of cells, reducing thereby the contamination of the plasma with cellular DNA which can interfere with the accuracy of the DNA analysis. Traditionally plasma is separated from blood by centrifugation or filtration. For the preparation of cfDNA an additional step of filtration or micro-centrifugation is often recommended to ensure that the plasma or serum is of a high purity²⁹. The DNA may be further purified by extraction before performing PCR. As yet there are no officially agreed standards for the purification of DNA from plasma, but the most common and fastest method is the QIAamp blood kit, which uses the binding of DNA to a silica gel membrane. Some studies claim however a 20% less recovery of cfDNA using this kit compared to other methods of DNA purification such as the Triton/Heat/Phenol (THP) protocol³⁰.

CfDNA loss during purification has been reported to occur due to the small fragment size³¹. These processing steps although necessary can also be slow and cumbersome. Moreover the generation of aerosols is common during centrifugation, which can be a potential risk of infection and contamination. Cell damage and cell loss is also a concern during centrifugation³². For point-of-care diagnostics, it is also well known that sample preparation step is a serious bottleneck in microfluidics.

The development of a miniaturised module capable of de-skilled blood separation would aid in the translation of this new technology.

The objective of this study was to investigate: (i) the influence of the entrance hematocrit and flow rate on the separation efficiency, (ii) the hematocrit and the cell-free zones, (iii) the purity of the plasma obtained using flow cytometry, (iv) the influence of the dilution of whole blood prior to on-chip separation and (v) the influence of the separation efficiency on the PCR efficiency. In order to prove the presence of biomarkers in the extracted plasma and to study the detection limits versus dilution levels and purity efficiency, we also performed a series of PCR reactions on human genes.

Theory and Design of a Blood Plasma Separator

The number of parameters affecting the flow of cells in a microchannel renders difficult the prediction of separation system behaviour. An earlier publication has discussed in details the presence and effects of viscous and inertial lift forces which enable particles to be separated at the microscale⁵. In a straight microchannel, deformable particles such as leukocytes move away from the walls under either the effect of inertial lift if the Reynolds number is close to 1 or by viscous lift when the Reynolds number is low. Both effects arise from the presence of a stationary wall and the interaction of a shear gradient on the particle. A transitional regime also exists where both effects may co-exist as discussed in^{5,33}. The cell-free layer observed on the walls at certain conditions depends also on the particle-particle interactions and the particle concentration. The design presented here exploits two main hydrodynamic effects: the Zweifach-Fung bifurcation law and the blood flow focusing effect occurring after a constriction. The Zweifach-Fung bifurcation law is an empirical law that addresses the deformable particle behaviour at a bifurcation³⁴. At a bifurcation, a cell will have the tendency to travel to the daughter channel with the highest flow rate, providing that the cell dimension is comparable to the channel dimension. Although this law was first stated in the context of microcirculation in the human body, it has also been exploited for in-vitro separation³⁵. From a few cells in a microvessel, the law was generalised to accommodate the situation where populations of cells flow in microchannels several tens of microns wide. The Zweifach-Fung effect is commonly used in the design of micro-separators to set up a lower limit for flow rate ratio at a bifurcation. However, the physics which underpin the law and its limitations are not clearly understood yet. The second effect is the focusing of the flow of red blood cells after a constriction. In⁵ the cell free layer of blood and the focusing of red blood cells after constriction were found to be small in a the 200 μ m wide microchannel. Faivre et al., reported better focus but used lower Reynolds number and therefore lower flow rate even at higher viscosity³. In this study we chose to keep the entrance flow rate high, and use inertial lift forces rather than viscous ones.

As shown in Figure 1, the design bears four connections, a single inlet for whole blood, one outlet for the concentrated cells and two outlets for the extracted plasma. Four plasma channels of 5.5mm in length are placed on each side of a 100 μ m wide main channel at a 45° angle. Meanders are used to minimize the area occupied by the eight plasma channels and keep the footprint of the chip low. A constriction has been placed before each of the plasma channels in order to create a cell-free zone from which the plasma is extracted. A set of chips has 20 μ m wide plasma channels while another has 10 μ m wide plasma channels. The depth of the microchannel networks is 20 μ m for all structures.

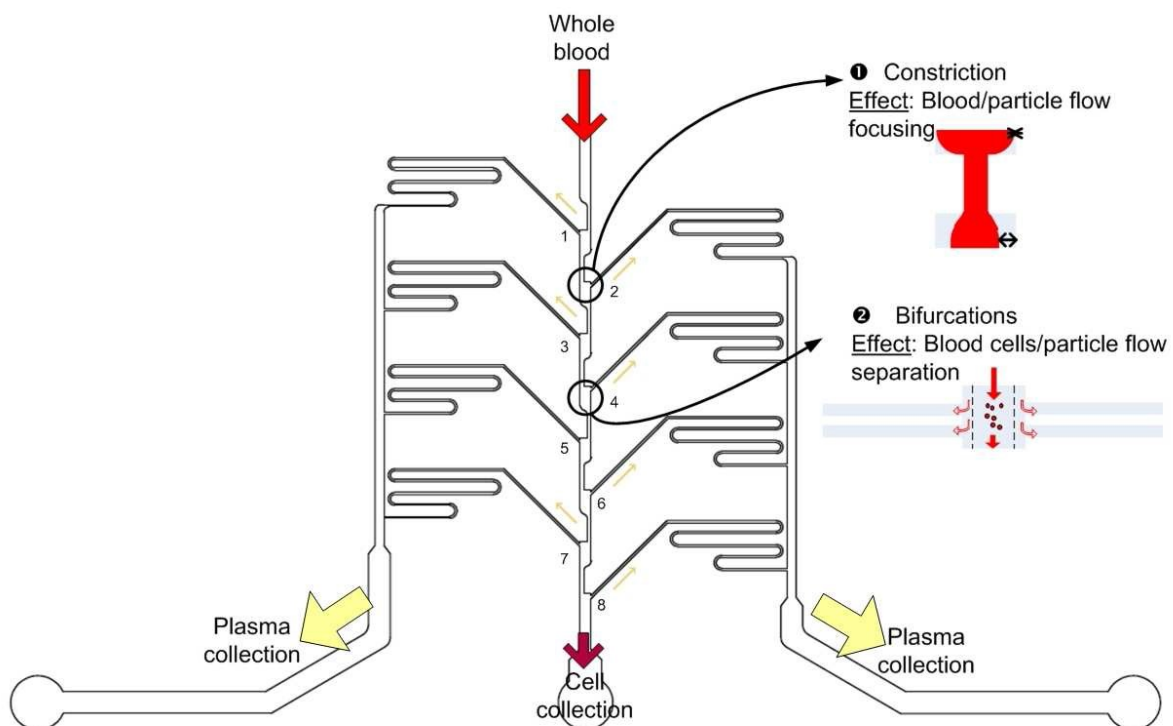


Figure 1. Schematic of a 20 μ m wide microchannel blood plasma separator. The flow of plasma is indicated by the yellow arrows.

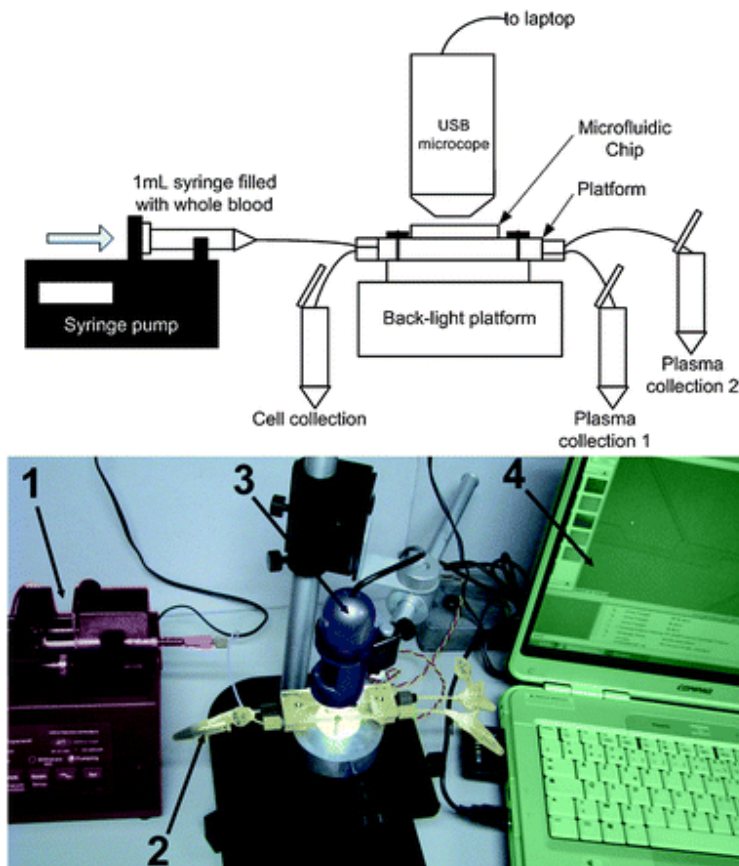
The plasma channels due to their geometrical features (length and width) have a high fluidic resistance value, whereas the main channel segment which has broader width and shorter length has lower resistance; this difference in resistance value at each bifurcation is proportional to the flow rate ratio. The value of the fluidic resistance of the main channel decreases after each bifurcation. Since the plasma channels have the same lengths the flow rate ratios are expected to be different at each bifurcation. The flow rate ratios can be roughly calculated by the Saber(TM) Microfluidic applications software (CoventorWare). Flow rate ratios have been calculated as approximately 17.8,

22.6, 31.8 and 55.6 for the left hand side of the chip (bifurcations 1, 3, 5, 7) and 19.2, 25.7, 40.1, and 94.5 for the right hand side of the chip (bifurcations 2, 4, 6, 8) with 20 μ m plasma channels. The side having the highest flow rate ratios is expected to perform better. Theoretically, the design should extract 30% of plasma for the 20 μ m design and 7% for the 10 μ m design.

Materials and methods

Microfluidic chip manufacturing

The microfluidic chips were manufactured by our industrial collaborator, Epigem Ltd (Redcar, UK). The chips consist of several sandwiched layers of the negative photoresist, SU8 between two PMMA layers, ensuring a “whole SU8” channel network. SU8 is patterned using conventional photolithography. Since the chip footprint is small (18mm x 23mm) a generic platform also made from an assembly of PMMA and SU8 is used as a holder featuring standard microfluidic connections (Cheminert) as shown in Figure 2.



← **Figure 2.** Photo of experimental set-up (1) Syringe pump and 1mL syringe loaded with blood. (2) Blood plasma separation chip device loaded with chip. Eppendorfs on the left collect blood cells, while eppendorfs on the right collect plasma (3) USB 5 Microscope (4) Laptop for visualisation.

Samples

Human blood was obtained in 500mL bags from the Scottish National Blood Transfusion Service, Lauriston Place, Edinburgh. Samples were used with the donors' prior consent and ethical clearance was obtained from the SNBTS Sample Governance Committee. Blood was treated with oxalate and stored at 4°C upon the day of reception. The blood was used within a month. Ideally the blood should be separated on the same day, and the PCR performed within hours after the separation. However, this could not be achieved in the current situation. This delay has been taken into account when interpreting the results. During the length of the study two different blood samples were obtained. The blood samples were subjected to different dilutions using Phosphate Buffered Saline, (PBS, Sigma). The dilution levels ranged from zero to 1:20. Dilution levels on different blood samples are biased by the intrinsic hematocrit of the blood donor at the time of the collection. Therefore, only resulting hematocrit levels truly reflect the different dilutions performed. Hematocrit level measurements and a full cell count were performed using a Beckmann Coulter Counter before each run.

Experimental set-up

The tests were performed at the Division of Pathway Medicine (DPM), University of Edinburgh (Royal Infirmary of Edinburgh, Little France, Edinburgh) in a level II biosafety facility. The chip was loaded onto the holder with microfluidic connections. The chip and holder assembly was placed onto a custom made back-light apparatus and examined under a digital microscope (DinoLite USB microscope, Big C, USA) to observe the flow and detect any obstacle to the flow path during each experiment. The flow was activated at flow rates ranging from 1mL/h to 10mL/hr (from 16.7 μ L/min to 167 μ L/min) by a syringe pump (Aladdin, WPI, USA). A syringe of 1mL (BD Plastipak) of blood was loaded for each experiment.

Microfluidic blood plasma separation

Around 50 μ L aliquots of each blood samples were placed in individual eppendorf tubes for hematocrit level verification using a Beckmann Coulter Counter. The microfluidic devices were prefilled before each experiment with a 1% BSA-PBS buffer for at least 10 minutes to avoid cell adhesion during the separation process³. Despite this prevention, the microfluidic network tends to clog up after at least three experiments due to platelets aggregations. If a blockage was spotted, or if the efficiency of the chip seemed to drop, the chip was discarded and a new one was loaded on the holder. The chips are meant to be low cost and disposable and should really be single-use. Once the blood samples filled the main channel, the separation process occurred at each bifurcation and the plasma flowed through the

individual plasma channels and collection channel. The cell enriched mixture and the extracted plasma were collected in three individual eppendorf tubes, as shown in Figure 2, and stored at 4°C until further processing.

Results

Separation efficiency

Influence of the entrance hematocrit and flow rate on the separation efficiency

The influence of entrance hematocrit on the separation efficiency was studied using different dilution levels. For the chip with the 20µm plasma channels, the corresponding hematocrit levels to the dilution levels were comprised between 3.3% and 31%. In the chip with the 10µm plasma channels, higher levels of hematocrit were studied, ranging from 9.4% to 45%. The purity efficiency was defined as:

$$E_p = 1 - \frac{c_p}{c_f}$$

Where c_p and c_f are the number of Red Blood Cells (RBCs) per mL in the plasma collection outlet and in the feed inlet, respectively.

Figure 4 shows the different purity efficiencies obtained as a function of the entrance hematocrit levels in the 20µm plasma channel microfluidic chip. Some hematocrit levels have several experimental points (two or four). Two points are due to the independent measurement of data from each plasma outlet. Four points are due to two different experiments, each of them having two different experimental points from each of the plasma outlets. Three different flow rates were used (2mL/h, 5mL/h and 10mL/h), hence figure 4 also measures the influence of flow rate on the separation efficiencies. At entrance hematocrit (eHCT) levels of 1.8% to 10%, the efficiency of the first plasma branch is comprised between 95% and 100%. For an entrance hematocrit greater than 10% the purity efficiency decreases regularly from approximately 95% to 32% for an eHCT of 33.7%. Hemoglobin levels recorded by the Cell Counter Coulter are also indicated here to report on the damage of the RBCs. The hemoglobin level can reach 100g/L for sample of eHCT of 33.7% processed at 5mL/hr. Below eHCT of 15% the hemoglobin level is below 20g/L. The total yield obtained by the 20µm wide channel design was approximately 30%.

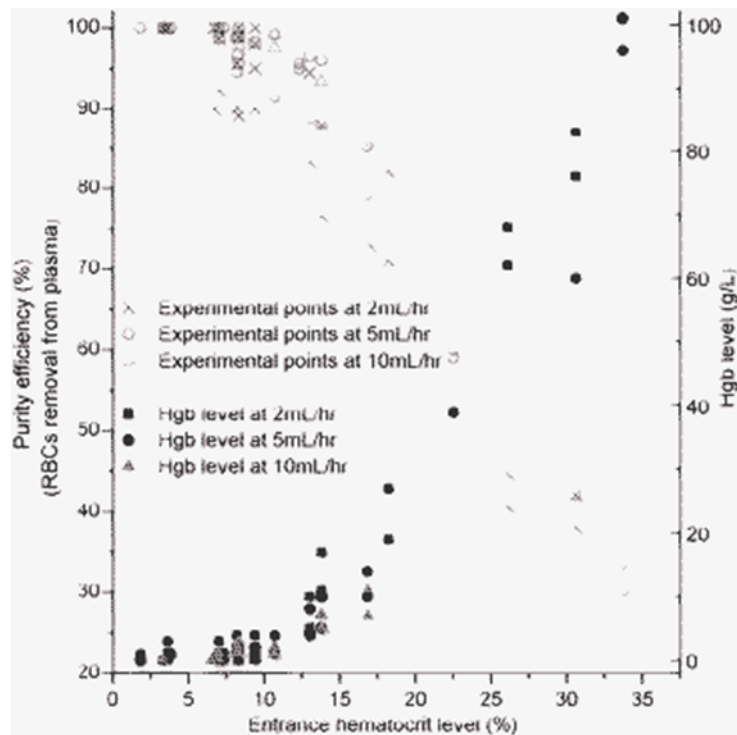


Figure 4. Influence of the hematocrit level on the purity efficiency and cell lysis in the 20 μ m wide plasma channels model at different blood flow rates.

Figure 5 details the results of the 10 μ m plasma channel chips. In these experiments the only flow rate used was 2mL/h. Again hemoglobin levels are indicated here to report on RBC damage. The hemoglobin levels are increasing with the hematocrit. However, it stays below the level reported to introduce interference with PCR reactions (5g/L)³⁸. The purity efficiency decrease very slightly (99%) towards hematocrit levels comparable to whole human blood, with plasma yield reaching 5%.

(turn to next page →)

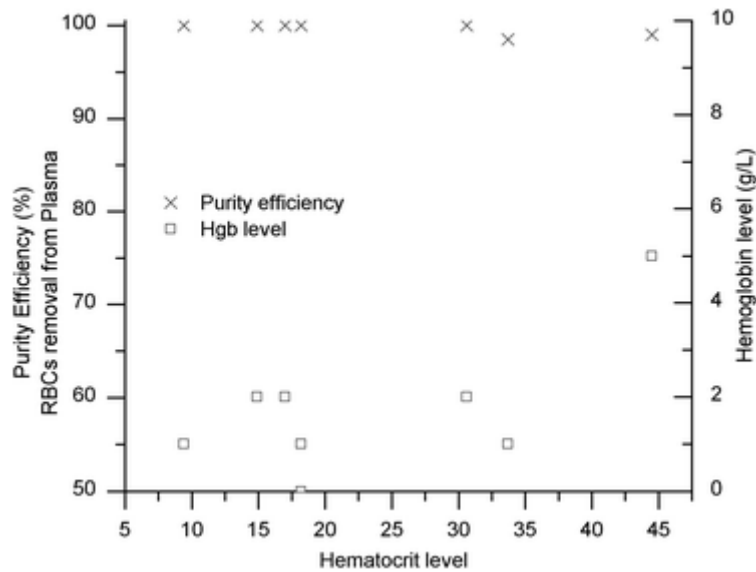


Figure 5. Influence of the hematocrit level on the purity efficiency and cell lysis in the 10 μ m wide plasma channels model for a flow rate of 2mL/hr.

Hematocrit and the cell-free zones

The influence of the eHCT on the cell-free zone was observed independently of the flow rate at each bifurcation. Figure 6 shows the dependence at bifurcation number 7 (location shown in Figure 1) of the cell-free zone on the entrance hematocrit level (eHCT). The lower the entrance hematocrit level, the larger is the cell free zone. As illustrated in Figure 6, the cell-free zone can be measured from the middle of the construction lateral dimension. From (a) to (b), the hematocrit is divided by 2, while the cell-free zone size is multiply by 2.5. For low hematocrit levels (8.3% and 3.3%) and a relatively high flow rate (here 10mL/hr) a recirculation pattern forms just after the constriction, while no recirculation is observed for a level of 16.8%. The lower the haematocrit level, the larger the recirculation pattern will be. The recirculation does not affect the separation efficiency at this flow rate, nor does it indicate the presence of turbulence. On the contrary it has been reported that recirculation may enhance the separation³⁹.

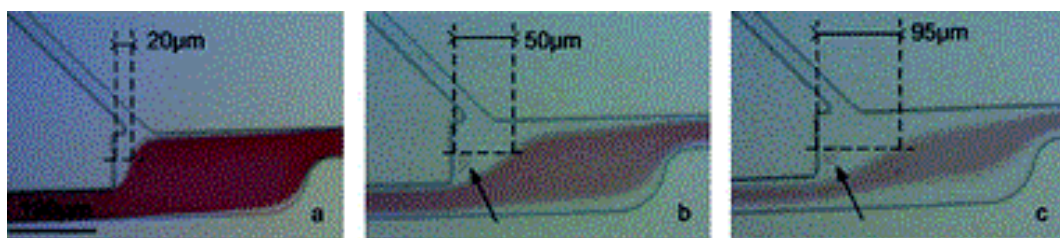


Figure 6. Effect of the entrance hematocrit level at bifurcation 7 for a constant flow rate of 10mL/hr, (a) eHCT=16.8 (b) eHCT=8.3 (c) eHCT=3.3. The arrow highlights the recirculation flow in (b) and (c).

Flow rate and the cell-free zones

In the same fashion, the influence of the flow rate on the cellfree zones has been observed. Three separation experiments were carried out with the same entrance hematocrit of 8.3% and varying flow rates of 2mL/h, 5mL/h and 10mL/h. The effect of the flow rate at the third bifurcation is shown in figure 7. Compared to the previous example, no recirculation eddies are observed at bifurcation number 3. The size of cell free zone here is approximately linear relative to the flow rate. However, more data would be needed to establish this linearity. A high flow rate ultimately leads to a higher purity but also increases the risk of damaging the cells through greater shear rate forces.

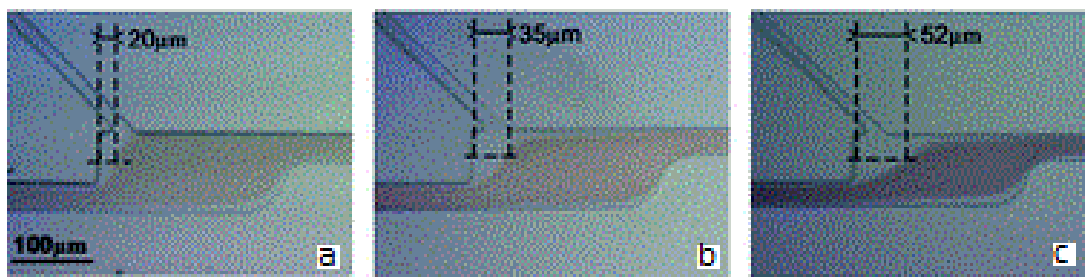


Figure 7. Effect of the flow rate at bifurcation 3, for an entrance HCT=8.3% (a) 2mL/hr (b) 5mL/hr (c) 10mL/hr. Note: the changes in colour are only due to camera settings at the time of the photograph.

Flow cytometric study

Motivation

A flow cytometric study was performed on several samples to get an in-depth knowledge of the separation of plasma from blood. Flow cytometry allows a very precise counting of particles in a fluid and, in this case, provides information on the cell population, such as cell lysis that may be caused by the high shear rates in the microchannels. Flow cytometry offers a higher level of sensitivity than can be achieved with a Coulter Counter. As the ultimate goal of the plasma separation is to detect cfDNA in the plasma, it is crucial to prove that the cells are not damaged/destroyed during separation.

Damaging the cells and causing lysis leads to more contamination of the plasma. In order to give useful biomedical information, the cfDNA detected in the plasma should be present in the blood prior to extraction and should not come from cell lysis as a result of sample preparation.

Experimental section

Staining of the blood sample was performed to label leukocytes and platelets. The R-phycoerythrin (R-PE)-conjugated monoclonal antibody CD45 (PE Mouse Anti-Human, BD Biosciences) was used for leukocytes surface staining. The fluorescein isothiocyanate (FITC)-conjugated CD42 antibodies stained the platelets. Using these markers we were able to identify the leukocytes and platelets population. The RBCs were identified by being non-stained. Blood cell population analysis was carried out on a FACS Scan instrument (BD Biosciences, Franklin Lakes, NJ, USA) and results were analysed using Flow Jo software v7.5.3 (Tree Star, Ashland, OR, USA). Determination of 5 the absolute cell count was achieved by the use of flow cytometric beads (Flow Count, Beckam).

Results

Figure 8 shows the results of the flow cytometric data after processing. The horizontal axis represents the size of the cells (Forward scatter, FSC) and the vertical axis represents their granularity (Side Scatter SSC). In the feed collection the population is mainly constituted of RBCs (95.62%), platelets (4.1%), leucocytes (0.28%), which corresponds to normal physiological conditions. Additionally the counting beads are present in the mixture, as well as the population identified as platelets aggregates and platelets-monocytes aggregates⁴⁰. The platelets are located in the bottom-left quadrant of the diagram, as they are the smallest particles and the least granular. In this quadrant a large population of red blood cells is also present; these are either very small RBCs or RBCs debris. The blood sample presents a large population of cell debris before any cell separation. A possible explanation for this is cell damage caused by the processing, transport and storage of the blood. Other RBCs, counting beads, monocytes and platelets aggregates can be found in the upper right quadrant. Linking these two quadrants is the “tail” of the healthy RBCs population, smaller or damaged RBCs. Little change is observed between the feed collection and the cell collection after separation. The tail does not show signs of growth which means that the cells have not been through high stress or have resisted the stress. Looking at the plasma collections, the plasma is not entirely devoid of cells, but has been strongly depleted by 250 times compared to the feed sample. Most of the RBCs debris has also been removed, which enhances the overall quality of the plasma. The population of platelets is the less depleted of all cell populations.

In conclusion, the flow cytometric investigation has shown that the cells are not damaged through the system. Additionally, the plasma is not entirely devoid of cells as the cell coulter counter suggests, but that the RBC population in the plasma collection has been reduced 250 times compared to the feed sample. Finally, the system also removes the cell debris, rendering the plasma even purer.

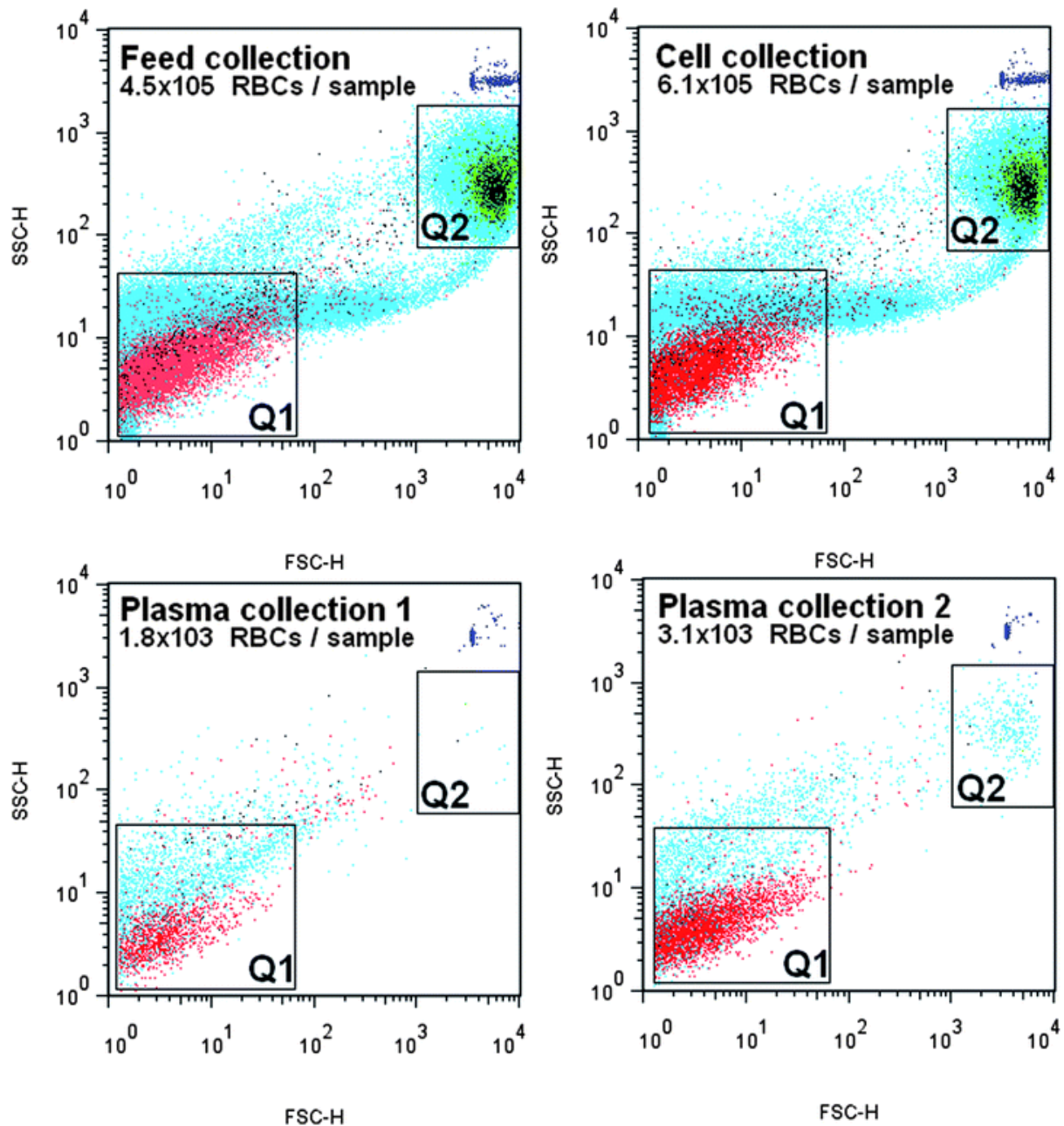


Figure 8. Dot plots of FSC vs. SSC represents the acquisition of 1000 flow check beads in the 250 μ L feed, cell, plasma 1 and plasma 2 collections. Colour correspondence: Dark blue: Flow Check beads, Black: leukocytes, Red: platelets, Light Blue: RBCs, Green: monocytes-platelets or platelets aggregates.

Detection of biomarkers

Of interest in this study is the subsequent recovery of cfDNA from the plasma after the on-chip blood plasma separation process. To assess the quality of the plasma extracted on-chip, PCR for a house-keeping gene was performed. The GAPDH gene was chosen for its small molecular weight (200bp)

which makes it a challenging target to amplify and also because its size is relative to cfDNA fragments¹⁹. The goal of this biological study is to prove that cfDNA can be amplified and detected in plasma obtained using this on-chip separation method. In order to investigate whether the dilution level prior to separation alters the recovery of biomarkers we studied the influence of pre-dilution on the PCR efficiency. The influence of the separation efficiency on the PCR efficiency has also been measured to characterise the limits of the separation method.

Conventional PCR and gel electrophoresis on house-keeping genetic sequences

The theoretical aspect of PCR has already been treated in a large body of literature^{41,42}. PCR was performed using a Primus 96 thermal cycler. In order to assess the suitability of on-chip blood separation as a module in a larger μ TAS system with minimal processing steps, no further purification was carried out on the plasma prior to PCR.

Amplification of house-keeping gene in the cell-free DNA population present in the plasma extracted on-chip

The amplification primers for the GAPDH gene (Forward primer 5'- GAA GGT GAA GGT CGG AGT CA-3', reverse primer 5' GAC AAG CTT CCC GTT CTC AG) were purchased from Metabion International AG. For the PCR with the GAPDH gene, each reaction aliquot contained 0.4 μ M forward primer, 0.4 μ M reverse primer, 0.1 μ M dNTP (Sigma), 80 0.1 μ M dCTP (Sigma), 2.5U Taq DNA polymerase (QIAGEN HotStarTaq DNA Polymerase kit), 2.5 μ L PCR buffer (HotStarTaq DNA Polymerase kit), 4mM MgCl₂ (QIAGEN HotStarTaq DNA Polymerase kit), 9 μ L DNA free water. For each reaction, 5 μ L of plasma was added to 20 μ L of the PCR master mix. In order to determine whether GAPDH could be amplified directly in whole blood, a control consisting of unpurified blood (as received from the blood bank) was measured. As a negative control for PCR, we used ultrapure water. Human genomic control DNA was used as a positive control and was obtained from Promega in 210ng/ μ L concentration, diluted 100 times. 1 μ L of 5 the dilution was added to the 20 μ L mastermix, with 4 μ L of DNA-free water to get a total of 2ng of DNA per reaction.

The thermal cycling program consisted of a 10min denaturation at 95°C, followed by 40 cycles of 1min denaturation at 94°C, 1min primer annealing at 68°C, 1min extension at 72°C. The final extension step consisted of a further 5min cycle at 72°C and the samples were kept on hold at 10°C until further processing. The PCR product was purified with the QIAGEN PCR purification kit using the protocol suggested by the manufacturer. The purified DNA product was eluted in 30 μ L EB buffer.

10 μ L of this product was then loaded onto a 2% agarose gel for analysis by electrophoresis. Gels were analysed using a Biorad Gel Doc system.

Influence of the dilution of whole blood previous to on-chip separation

PCR was performed to detect the GAPDH gene in the plasma samples extracted on-chip. Samples were isolated after separation and stored in 1mL eppendorf tubes at 4°C prior to use. The separation efficiency was characterised by a Coulter Counter as described previously. In order to assess the influence of the dilution on the PCR efficiency, six samples with the same separation efficiency but different dilution levels (eHCT level varying from 3.3% to 33.7%) were chosen. Achieving the same separation efficiency with different pre-diluted samples is possible through the use of the two chip models and different flow rates. PCR and gel electrophoresis were performed on these 15 samples, following the protocol presented in the previous section. Samples S1 to S6 were duplicated to verify the homogeneity of the PCR. Table 1 summarises the different samples and controls used in this first experiment.

		Separation efficiency of sample (%)	Entrance hematocrit level (%)
Samples	S1	100	3.3
	S2	100	6.2
	S3	100	7.0
	S4	100	14.9
	S5	100	17
	S6	100	33.7
Positive controls	G1	<i>Genomic control 1 – 1/10</i>	
	G2	<i>Genomic control 2 – 1/100</i>	
	G3	<i>Genomic control 3 – 1/1000</i>	
Other controls	WB	<i>Whole blood</i>	
	C	<i>Plasma sample extracted by gentle centrifugation (3000 rpm, 10 min)</i>	
Negative control	W	<i>Ultrapure water</i>	

Table 1. Table summarising the characteristics of the samples and controls.

The amplified products of the plasma samples are shown in Figure 9. In all columns except the one of the negative control, a clear 200bp band is present, showing the consistent amplification of the GAPDH gene fragment. The intensity of the band varies from sample to sample, but the intensity does not vary within the duplicates. Both samples in series 1 show a relatively strong amplification band. Interestingly, there is a broad trend towards higher fluorescence signal from S1 to S6, (excluding S5)

which confirms, as expected, that the resulting concentration achieved by PCR amplification depends on the entrance hematocrit of the sample. Additionally, the presence of an amplification band in the sample with the highest dilution (corresponding hematocrit level 3.3%) demonstrates that PCR can be achieved on strongly diluted samples. All the other controls, including the negative controls show no amplification. for the lanes containing the whole blood product (WB), and the plasma extracted by centrifugation (C), the PCR has been inhibited, probably by the presence of immunoglobulin G in the whole blood and in the plasma sample extracted by centrifugation. To the best of our knowledge, this is the first demonstration of PCR on cfDNA in plasma extracted on chip.



Figure 9. Ethidium bromide-stained agarose gel of PCR products obtained with GAPDH primer and unprepared plasma samples obtained by microfluidic extraction. The first lane is a molecular weight marker (1000-bp ladder).

Influence of the separation efficiency on the PCR efficiency

As demonstrated by Figure 9, PCR can be achieved on cfDNA in plasma extracted on-chip for purity efficiency of 100%. Further study was carried out to assess the limits of the PCR capability on cfDNA in untreated plasma sample. In that respect, plasma aliquots from samples with similar entrance hematocrit levels and with different purity efficiencies were collected after separation and stored at 4°C. The different samples used in this experiment are presented in Table 2. The separation efficiency of the samples ranged from 65.1% to 100%.

		Separation efficiency (%)	Hematocrit level (%)
Plasma samples	S1	100	14.9
	S2	97.8	12.3
	S3	94.9	12.3
	S4	84	16
	S5	65.1	16
Positive controls	G1	<i>Genomic control 1 – 1/10</i>	
	G2	<i>Genomic control 2 – 1/100</i>	
	G3	<i>Genomic control 3 – 1/1000</i>	
Other control	WB	<i>Whole blood control</i>	
Negative control	W	<i>Ultrapure water</i>	

Table 2. Different samples used in the PCR experiment.

The amplified products of this experiment are shown in ethidium bromide-stained agarose gel in Figure 10. A clear gradient of band intensity through samples S1 to S5 can be observed. No PCR product could be amplified from S5 which has a purity efficiency of 65.1% and the band from S4 (84%) is visible but faint. The whole blood and water lanes did not show any amplification.

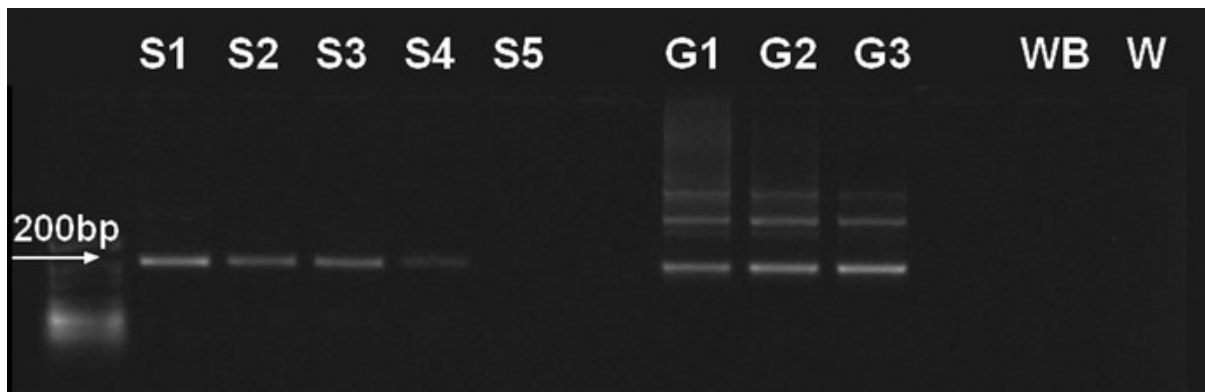


Figure 10. Influence of the separation efficiency on the detection of the GapDH house-keeping gene in the on-chip extracted plasma. The first lane is a molecular weight marker (50bp ladder).

This experiment demonstrates that the PCR efficiency depends on the separation efficiency, and most importantly shows that at the high separation efficiencies which are standard for our device, PCR can be routinely performed. Moreover these experiments successfully showed that the plasma

extracted on-chip is pure enough to perform amplification without further purification steps as routinely done after centrifugation today, reducing reagent costs, waste and time. It can be noted that for more difficult cfDNA targets such as cffDNA, this step might still be necessary.

One final and important point to consider is the effect of the time delay between draw and processing of blood which has been shown to be a factor in the quantification of cfDNA. Lysis of intact cells caused by a delay in blood processing would result in increased concentrations of cfDNA (caused by ex-vivo processing) which might lead to misleading results especially if cfDNA is used as a biomarker in cancer, prenatal and post transplant care. Integrating the process of blood plasma separation and PCR analysis onto a single chip would overcome this limitation for the routine use of cfDNA analysis in clinical settings.

Conclusions

This paper demonstrates an efficient and disposable way to extract at high flow rate cell-free plasma from whole blood at different dilution levels. The purity efficiency reached 100% even with the use of relatively large channels ($20\mu\text{m}$) suitable for mass manufacturing. PCR was used to demonstrate the purity of the extracted plasma without the need for DNA extraction. To the best of our knowledge, we describe for the first time the recovery of cell-free DNA from on-chip extracted plasma by PCR and gel electrophoresis. As expected, the detection nucleic acids biomarker depends on the separation efficiency, but also on the dilution of the blood. Detection was demonstrated in plasma samples with purity efficiency from 84% and dilution level up to 1:20. All our findings indicate that this continuous microfluidic separation system may be used as a preliminary module to a lab-on-chip system.

References

- [1] J.V. Zoval, M.J. Madou, *Proc. IEEE*, 2004.
- [2] T. Brenner, T. Glatzel, R. Zengerle, J. Ducree, Proceedings of the micro Total Analysis Conference, California, 2003.
- [3] M. Faivre, M. Abkarian, K. Bickraj, S. Howard, *Biorheology*, 2006, **43**,147-159
- [4] A.I. Rodríguez-Villarreal, M. Arundell, M. Carmona and J. Samitier, *70 Lab Chip*, 2010, DOI: 10.1039/b904531g
- [5] M. Kersaudy-Kerhoas, R.S. Dhariwal, M.P.Y. Desmulliez, and L. Jouvét, *Microfluidics and nanofluidics*, 2010, 8, 105-114
- [6] *Br. Pat.*, IPO 310809, 2009.
- [7] S.A. Leon, B. Shapiro, D.M. Sklaroff and M.J. Yaros, *Cancer Res.*,75 1977, **37**, 646–650
- [8] H. Schwarzenbach, C. Alix-Panabières, I. Müller, N. Letang, J.P. Vendrell, X Rebillard, and K. Pantel, *Clin Cancer Res.* 2009, **15**, 1032-8.
- [9] O. Gautschi, C. Bigosch, B. Huegli, M. Jermann, A. Marx, E., Chasse, D. Ratschiller, W. Weder, M. Joerger, D.C. Betticher, R.A. Stahel , and A. Ziegler. *Clin Onc*, 2004, **22**, 4157–64.
- [10] M. Fleischhacker, B. Schmidt, *Biochim Biophys Acta*, 2007, **1775**, 181232.
- [11] F. Diehl, M. Li, D. Dressman, Y. He, D. Shen, S. Szabo, et al. *Proc Natl Acad Sci U S A*, 2005, **102**, 16368 –73
- [12] B. Shapiro, M. Chakrabarty, E.M. Cohn, S.A. Leon, *Cancer*, 1983, **51**, 2116.
- [13] V. García Moreira, B. Prieto García, J.M. Baltar 5 Martín, F. Ortega Suárez, F.V. Alvarez, *Clin. Chem.*, 2009, **55**, 1958 - 1966
- [14] Y.M.D. Lo, *J. Histochem. Cytochem*, 2005, **53**, 293.
- [15] J.M. Costa, P. Ernault, *Clin Chem.*, 2002, **48**, 679.
- [16] K.M. Finning, P.G. Martin, P.W. Soothill, N.D. Avent, *Transfusion*, 2002, **42**, 1079.
- [17] C. Wright, PHG Foundation. (2009) <http://www.phgfoundation.org/pages/ffdna.html>
- [18] X.Y. Zhong, W. Holzgreve, S. Kahn. *Hypertens Pregnancy* 2002, **21**, 77.

- [19] S. Jahr, H. Hentze, S. Englisch, D. Hardt, F.O. Fackelmayer, R.D. Hesch and R. Knippers, *Cancer Res*, 2001, **61**, 1659 – 1665.
- [20] A. Sekizawa, M. Jimbo, H. Saito, M. Iwasaki, Y. Sugito, Y. Yukimoto et al. *Clin Chem* 2002, **48**, 353–354.
- [21] Y. Ohashi, N. Miharu, H. Honda, O. Samura, K. Ohama., *Clin. Chem*, 2002, **48**, 386–388.
- [22] E.K. Ng, N.B. Tsui, T.K. Lau, T.N. Leung, R.W. Chiu, N.S. Panesaret al.. *Proc Natl Acad Sci USA*, 2003, **100**, 4360–4362.
- [23] P. Anker, M. Stroun. *Medicina (B Aires)*, 2000, **60**, 699-702
- [24] M. Stroun, P. Anker, J. Lyautey, C. Lederrey, and P.A. Maurice,
- [25] *Eur J Cancer Clin Oncol*, 1987, **23**, 707–712.
- [25] H.D. Halicka, E. Bedner, and Z. Darzynkiewicz. *Exp Cell Res*, 2000, **260**, 248–256.
- [26] Y.M.D. Lo, M.S. Tein, T.K. Lau, C.J. Haine, T.N. Leung, P.M. Poon. *Am J Hum Genet*, 1998, **62**, 768.
- [27] D. W. Bianchi, *Trophoblast Research*, 2004, 18, S93–S101.
- [28] A.W. Al-Soud, L.J. Jönsson, and P. Rådström, *J. Clin. Microbiol.*, 2000, **38**, 345-350.
- [29] R.W.K. Chiu, L.L.M. Poon, T.K. Lau, T.N. Leung, E.M.C. Wong, and Y.M.D. Lo. *Clin Chem* 2001, **47**, 1607–1613.
- [30] X. Xue, M.D. Teare, I. Holen, Y.M. Zhu, and P.J. Woll, *Clin Chim Acta*. 2009, **404**, 100-104.
- [31] B. Schmidt, S. Weickmann, C. Witt, and M. Fleischhacker, *Clin Chem*, 2005, **51**, 1561–1563.
- [32] G. Sitar, L. Manenti, A. Farina, V. Lanati, P. Mascheretti, A. Forabosco, L. Montanari and E. Ascari, *Haematologica*, 1997, **82**, 5.
- [33] D. Di Carlo, J.F. Edd, D Irimia, R.G. Tompkins, and M. Toner, *Anal. Chem.*, 2008, **80**, 2204-2211.
- [34] Fung, Y.C., in *Biomechanics*, 2004, Springer.
- [35] S.S. Shevkoplyas, S.C. Gifford, T. Yoshida, and M.W. Bitensky, *Microvascular Research*, 2003, **65**, 132–136.

- [36] P. Olla, *J. Phys. II*, 1997 , **7**, 1533-1540.
- [37] R. Fan, O. Vermesh, A. Srivastava, B.K H Yen, L. Qin, H. Ahmad,G. A Kwong, C.-C. Liu, J. Gould, L. Hood and J. R Heath, *Nature Biotechnology*, 2008, **26**, 1373-1378.
- [38] V. VanDelinder, A. Groisman, *Anal Chem.*, 2006, **78**, 3765-3771.
- [39] E. Sollier, H. Rostaing, P. Pouteau, Y. Fouillet and J.L. Achard, *Sensors and Actuators B: Chemical*, 2009, **141**, 617-624.
- [40] Yoshimura Y, Y. Hiramatsu, Y. Sato, S. Homma, Y. Enomoto, Y. Kikuchi, andY. Sakakibara, *Ann Thorac Surg* 2003, **75**, 1254–1260.
- [41] D.G. Remick, S.L. Kunkel, E.A. Holbrook et al., *Am J. Clin. Path*, 1990, **93**, S49-S54.
- [42] P.A. Wright, D. Wynfordthomas, *J. Pathology* 1990, **162**, 99-117.